PHYSICAL REVIEW D **94,** 045022 (2016)

Influence of boson mass on chiral phase transition in QED_3

Hong-tao Feng,[1,4,*] Xiu-Zhen Wang,[1] Xin-hua Yu,[2] and Hong-shi Zong[3,4,†]

[1]*Department of Physics, Southeast University, Nanjing 211189, China*

[2]*School of Information and Communication, Guilin University of Electronic Technology, Guilin, Guangxi 541004, China*

[3]*Department of Physics, Nanjing University, Nanjing 210093, China*

[4]*State Key Laboratory of Theoretical Physics, Institute of Theoretical Physics, CAS, Beijing 100190, China*

(Received 31 August 2015; published 31 August 2016)

Based on the truncated Dyson-Schwinger equations for the fermion propagator with N fermion flavors at zero temperature, the chiral phase transition of quantum electrodynamics in $2+1$ dimensions (QED_3) with boson mass—which is obtained via the Anderson-Higgs mechanism—is investigated. In the chiral limit, we find that the critical behavior of QED_3 with a massless boson is different from that with a massive boson: the chiral phase transition in the presence of a nonzero boson mass reveals the typical second-order phase transition, at either the critical boson mass or a critical number of fermion flavors, while for a vanishing boson mass it exhibits a higher than second-order phase transition at the critical number of fermion flavors. Furthermore, it is shown that the system undergoes a crossover behavior from a small number of fermion flavors or boson mass to its larger one beyond the chiral limit.

DOI: 10.1103/PhysRevD.94.045022

I. INTRODUCTION

Quantum electrodynamics in $2+1$ dimensions (QED_3) has been widely studied for many years. It has many features similar to QCD, such as dynamical chiral symmetry breaking (DCSB) in the massless fermion limit and confinement [1–5]. Moreover, QED_3 is super-renormalizable, so it does not suffer from the ultraviolet divergence which is present in QED_4. Therefore it can serve as a toy model of more realistic theories such as QCD. Besides, QED_3 has been used to study some problems in condensed matter physics. In particular, QED_3 can be regarded as a model for high-T_c superconductivity and the fractional quantum Hall effect [6–10].

The research of the chiral phase transition (CPT) in QED_3 is an active subject, since Appelquist *et al.* [11] pointed out that QED_3 with N fermion flavors undergoes a CPT into the phase of DCSB when N is smaller than a critical fermion flavor N_c (≈ 3.24). They arrived at this conclusion by applying the lowest-order approximation of the truncated Dyson-Schwinger equation (DSE). Then, some groups adopted an improved scheme of the DSE and verified the existence of N_c [12,13]. In particular, the result of Ref. [13] illustrates that the critical behavior of the chiral fermion condensate obtained using the rainbow approximation of the DSE near N_c is the same as that obtained using the truncated scheme of the Ball-Chiu/Curtis-Pennington vertex [14,15]. The comparability implies that the rainbow approximation of the DSE can be used to qualitatively study the CPT in QED_3.

To determine the order of the CPT around N_c, the authors of Ref. [16] studied the light scalar degrees of freedom and the order parameter of the CPT near N_c and found that the phase transition is not second order and is also unlike the conventional first-order transition [17]. In addition, the results from the Cornwall-Jackiw-Tomboulis (CJT) effective potential [18] and chiral susceptibility [19] also show that the CPT around N_c with a *massless boson* at zero temperature is neither of first order nor of second order, and thus it should be a continuous phase transition of a higher order.

The above result about the nature of the CPT holds when the gauge boson is massless, but it is expected to change when the gauge boson gains a nonzero mass ζ. DCSB in QED_3 is a low-energy phenomenon and exists only in the infrared region, in which the gauge interaction is strong enough to cause fermion condensation. This requires the fermions to be apart from each other. However, when the gauge boson has a finite mass it cannot mediate a long-range interaction. This physical picture is obviously different from that with a massless boson which mediates a long-range interaction. The previous works showed that, with the involved boson mass, N_c depends apparently on the value of ζ [20,21]. Thus it is very interesting to investigate whether or not the characteristic of the CPT is also changed when including ζ and what will happen beyond the chiral limit.

In principle, we should adopt the Landau theory of phase transitions to study the nature of the CPT, but it is too complicated to expand the free energy of the system on the order of the CPT near the critical point. Fortunately, the chiral susceptibility contains some essential characteristics of the CPT. Moreover, the CJT effective potential [22] also

*fenght@seu.edu.cn
†zonghs@nju.edu.cn

provides us with a virtual framework to analyze the nature of the phase transition; thus, in this paper we shall adopt the two methods to analyze the critical behaviors of QED_3 with massless and massive bosons.

II. ORDER OF THE CHIRAL PHASE TRANSITION

The Lagrangian for massless QED_3 with N fermion flavors in a general covariant gauge in Euclidean space can be written as

$$\mathcal{L} = \sum_{j=0}^{N} \overline{\psi}_j(\partial + ieA - m)\psi_j + \frac{1}{4}F_{\sigma\nu}^2 + \frac{1}{2\xi}(\partial_\sigma A_\sigma)^2, \quad (1)$$

where the four-component spinor ψ is the massless fermion field, and ξ is the gauge parameter. In the absence of the mass term $m\overline{\psi}\psi$, this system has chiral symmetry and the symmetry group is $U(2)$. The original $U(2)$ symmetry reduces to $U(1)\times U(1)$ when the massless fermion acquires a nonzero mass due to nonperturbative effects.

It is different from the gauge field in the reformulated Thirring model in three dimensions [23], which was studied using the hidden local symmetry technique which reveals a gauge field character. In this work, we want to stress that the gauge boson in QED_3 will acquire a mass through the Anderson-Higgs mechanism which happens when the gauge field interacts with some scalar field in the phase with spontaneous gauge symmetry breaking. In physics, this phenomenon occurs in the state of plane superconductivity where spontaneous gauge symmetry breaking appears.

To see the effect played by ζ, we now introduce an additional interaction term between the gauge field A_μ and the complex scalar boson field ϕ:

$$\mathcal{L}' = \mathcal{L} + \mathcal{L}_B,$$
$$\text{with} \quad \mathcal{L}_B = \sum_{j=0}^{N}[|(\partial_\mu + ieA_\mu)\phi_j|^2 - \mu|\phi_j|^2 - \lambda|\phi_j|^4]. \quad (2)$$

$\mathcal{L}_B$ is the so-called Abelian Higgs model or relative Ginzburg-Landau model [24,25]. The scalar field ϕ represents the bosonic holons based on the spin-charge separation picture, while the coefficient λ is always positive according to the Landau phase transition theory. Physically, at $\mu > 0$, the system stays in the normal state and the vacuum expectation value of the boson field $\langle\phi\rangle = 0$, so the Lagrangian respects the local gauge symmetry. When $\mu < 0$, the system enters the superconducting state and the boson field develops a finite expectation value $\langle\phi\rangle \neq 0$; then, the local gauge symmetry is spontaneously broken and the gauge field acquires a finite mass ζ after absorbing the massless Goldstone boson. The finite gauge field mass is able to characterize the achievement of superconductivity. On the other hand, the gauge field obtains a mass via the Anderson-Higgs mechanism which implies that the gauge field is in a confinement phase [26], and thus the spinons and holons are confined in the superconducting phase (the spin-charge recombination). It is well known that neither spinons nor holons can be observed in high-T_c superconducting experiments; however, a well-defined quasiparticle can be observed due to the spin-charge recombination in the superconducting phase [27].

In this paper, we will follow Refs. [24–27] to add the gauge mass by hand and study the influence of ζ on the nature of the CPT in QED_3. The order of the CPT is defined via the full fermion propagator

$$\langle\overline{\psi}\psi\rangle = \mathrm{Tr}[S(x\equiv 0)] = \int \frac{d^3p}{(2\pi)^3}\frac{4B(p^2)}{A^2(p^2)p^2 + B^2(p^2)}, \quad (3)$$

which is related to the full fermion propagator $S(p)$ and reduces to its free one $S_0(p)$,

$$S^{-1}(p) = i\gamma\cdot pA(p^2) + B(p^2) \to S_0^{-1} = i\gamma\cdot p + m, \quad (4)$$

in the high-energy limit. It is well defined in the chiral limit, but it is divergent at $m \neq 0$. This divergence is typically removed and we obtain a renormalized fermion chiral condensate $\mathrm{Tr}[S(x\equiv 0) - S_0(x\equiv 0)]$.

A. Chiral susceptibility

We can also determine the transition point via the maximum of the chiral susceptibility $\frac{\partial\langle\overline{\psi}\psi\rangle}{\partial m}$ which indicates that the chiral susceptibility measures the response of the chiral condensate to an infinitesimal change of the fermion mass [28],

$$\chi^c = 4\int \frac{d^3p}{(2\pi)^3}\left\{\frac{p^2A^2D - 2p^2ABC - B^2D}{[p^2A^2 + B^2]^2} - \frac{p^2 - m^2}{(p^2+m^2)^2}\right\}, \quad (5)$$

where

$$C(p^2) = \frac{\partial A(p^2)}{\partial m}, \qquad D(p^2) = \frac{\partial B(p^2)}{\partial m}. \quad (6)$$

Now let us turn to the calculation of $A(p^2)$, $B(p^2)$ and the related $C(p^2)$, $D(p^2)$ functions which can be obtained by solving DSEs for the fermion propagator,

$$S^{-1}(p) = S_0^{-1}(p) + \int \frac{d^3k}{(2\pi)^3}[\gamma_\sigma S(k)\Gamma_\nu(p,k)D_{\sigma\nu}(q)], \quad (7)$$

where $\Gamma_\nu(p,k)$ is the full fermion-photon vertex and $q = p - k$. The simplest and most commonly used truncated scheme for the DSEs is the rainbow approximation,

i.e., $\Gamma_\nu(p,k) \to \gamma_\nu$, since it gives us rainbow diagrams in the fermion DSE and ladder diagrams in the Bethe-Salpeter equation for the fermion-antifermion bound-state amplitude [3–5]. The coupling constant $\alpha = e^2$ has dimension one and provides us with a mass scale. For simplicity, in this paper, mass and momentum are all measured in units of α, namely, we choose a kind of natural units in which $\alpha = 1$.

From Eqs. (4) and (7), we obtain the equations satisfied by $A(p^2)$ and $B(p^2)$,

$$A(p^2) = 1 - \frac{1}{4p^2}\int \frac{d^3k}{(2\pi)^3}\mathrm{Tr}[i(\gamma p)\gamma_\sigma S(k)\gamma_\nu D_{\sigma\nu}(q)], \quad (8)$$

$$B(p^2) = \frac{1}{4}\int \frac{d^3k}{(2\pi)^3}\mathrm{Tr}[\gamma_\sigma S(k)\gamma_\nu D_{\sigma\nu}(q)]. \quad (9)$$

Another involved function is the full gauge boson propagator $D_{\sigma\nu}(q)$ which is given by [20,29]

$$D_{\sigma\nu}(q) = \frac{\delta_{\sigma\nu} - q_\sigma q_\nu/q^2}{q^2[1+\Pi(q^2)] + \zeta^2} + \xi\frac{q_\sigma q_\nu}{q^4}, \quad (10)$$

where $\Pi(q^2)$ is the vacuum polarization for the gauge boson which is satisfied by the polarization tensor

$$\Pi_{\sigma\nu}(q^2) = -\int \frac{d^3k}{(2\pi)^3}\mathrm{Tr}[S(k)\gamma_\sigma S(q+k)\gamma_\nu] \quad (11)$$

and ζ is the gauge boson mass which is acquired through the Higgs mechanism, which happens when the gauge field interacts with a scalar field in the DCSB phase (more details about the Higgs mechanism in QED_3 can be found in Refs. [29,30]).

Using the relation between the vacuum polarization $\Pi(q^2)$ and $\Pi_{\sigma\nu}(q^2)$,

$$\Pi_{\sigma\nu}(q^2) = (q^2\delta_{\sigma\nu} - q_\sigma q_\nu)\Pi(q^2), \quad (12)$$

we can obtain an equation for $\Pi(q^2)$ which has an ultraviolet divergence. Fortunately, it is present only in the longitudinal part and proportional to $\delta_{\sigma\nu}$. This divergence can be removed by the projection operator

$$\mathcal{P}_{\sigma\nu} = \delta_{\sigma\nu} - 3\frac{q_\sigma q_\nu}{q^2}, \quad (13)$$

and then we obtain a finite vacuum polarization [31,32].

Finally, since the Landau gauge is the most convenient and commonly used one, we choose to work in the Landau gauge and immediately obtain the truncated DSEs for the fermion propagator and then analyze the critical behavior in this Higgs model.

By some tricks proposed in Ref. [9], we obtain the equations satisfied by $A(p^2)$, $B(p^2)$, and $\Pi(q^2)$,

$$A(p^2) = 1 + \frac{2}{p^2}\int \frac{d^3k}{(2\pi)^3}\frac{A(k^2)(pq)(kq)/q^2}{H(k^2)[q^2(1+\Pi(q^2)) + \zeta^2]}, \quad (14)$$

$$B(p^2) = m + 2\int \frac{d^3k}{(2\pi)^3}\frac{B(k^2)}{H(k^2)[q^2(1+\Pi(q^2)) + \zeta^2]}, \quad (15)$$

$$\Pi(q^2) = \frac{2N}{q^2}\int \frac{d^3k}{(2\pi)^3}\frac{A(k^2)A(p^2)}{H(k^2)H(p^2)} \times [2k^2 - 4(k\cdot q) - 6(k\cdot q)^2/q^2], \quad (16)$$

with $H(k^2) = A^2(k^2)k^2 + B^2(k^2)$.

Adopting Eqs. (6) and (14)–(16) and setting $\Pi'(q^2) = \frac{\partial\Pi(q^2)}{\partial m}$, we get the coupled equations for $C(p^2), D(p^2)$, and $\Pi'(q^2)$,

$$C(p^2) = \frac{2}{p^2}\int \frac{d^3k}{(2\pi)^3}\frac{(p\cdot q)(k\cdot q)\mathcal{C}}{H^2(k^2)[q^2(1+\Pi(q^2)) + \zeta^2]^2}, \quad (17)$$

$$D(p^2) = 1 + 2\int \frac{d^3k}{(2\pi)^3}\frac{q^2\mathcal{D}}{H^2(k^2)[q^2(1+\Pi(q^2)) + \zeta^2]^2}, \quad (18)$$

$$\Pi'(q^2) = \frac{2N}{q^2}\int \frac{d^3k}{(2\pi)^3}\frac{[2k^2 - 4(k\cdot q) - 6(k\cdot q)^2/q^2]\Pi_1'}{H^2(k^2)H^2(p^2)}, \quad (19)$$

where

$$\begin{aligned}
\mathcal{C} \equiv{}& [B^2(k^2)C(k^2) - A^2(k^2)C(k^2)k^2 - 2A(k^2)B(k^2)D(k^2)] \\
&\times [1 + \Pi(q^2) + \zeta^2/q^2] - A(k^2)H(k^2)\Pi'(q^2), \\
\mathcal{D} \equiv{}& [A(k^2)D(k^2)k^2 - B^2(k^2)D(k^2) - 2A(k^2)B(k^2)C(k^2)k^2] \\
&\times [1 + \Pi(q^2) + \zeta^2/q^2] - B(k^2)H(k^2)\Pi'(q^2), \\
\Pi_1' \equiv{}& [A(p^2)C(k^2) + A(k^2)C(p^2)]H(k^2)H(p^2) \\
&- 2A(k^2)A(p^2)[A(k^2)C(k^2)k^2 + B(k^2)D(k^2)]H(p^2) \\
&- 2A(k^2)A(p^2)[A(p^2)C(p^2)p^2 + B(p^2)D(p^2)]H(k^2).
\end{aligned}$$

B. CJT effective potential

Furthermore, to indicate the order of the *CPT* with the gauge boson mass, we can also analyze the derivative of the generating functional with respect to the number of fermion flavors and the boson mass. Due to its nonperturbative nature, it is too complex to obtain an exact expression for the generating functional. However, in some situations, an expression for the effective potential can be given in terms of the fermion and boson propagators (which correspond to the bare vertex approximation for solving the DSEs for the

fermion and boson propagators) to study the nature of the chiral phase transition around the critical point.

The pressure is the negative value of the CJT effective potential density and the CJT effective pressure is given as [22]

$$\mathcal{P}(\zeta,N)=-N\mathrm{Tr}\left[\ln(SS_0^{-1})+\frac{1}{2}(1-SS_0^{-1})\right]+\frac{1}{2}\mathrm{Tr}[\ln(DD_0^{-1})+(1-DD_0^{-1})], \tag{20}$$

where the trace, logarithm, and propagators are taken in the functional framework. The first term represents the contribution of N fermion flavors, and the last term denotes the contribution of the photon. Because of the divergent integral, the differential pressure between the DCSB phase (d) and chiral restored phase (c) is often calculated as

$$\Delta\mathcal{P}(\zeta,N)=\mathcal{P}_d-\mathcal{P}_c \tag{21}$$

to determine which phase exists; this expression is reduced as

$$\Delta\mathcal{P}(\zeta,N)=-2N\int\frac{\mathrm{d}^3p}{(2\pi)^3}\left[\ln\frac{A_c^2p^2}{A_d^2p^2+B_d^2}+\frac{(A_d^2-1)A_d^2p^2+B_d^2}{A_d^2p^2+B_d^2}+\frac{1-A_c}{A_c}\right]+\int\frac{\mathrm{d}^3p}{(2\pi)^3}\left[\ln\frac{1+\Pi_c}{1+\Pi_d}+\frac{\Pi_d-\Pi_c}{(1+\Pi_d)(1+\Pi_c)}\right]. \tag{22}$$

The unknown functions in Eq. (22) can be obtained from Eqs. (14)–(16) both in the DCSB phase ($B>0$) and the chiral symmetric phase ($B\equiv 0$) in the chiral limit.

To indicate the nature of the CPT at the critical point, we can expand $\Delta\mathcal{P}(\zeta,N)$ by ζ (N) with a fixed N (ζ),

$$\Delta\mathcal{P}_N(\zeta)=\sum_{n=0}^{\infty}\frac{(\zeta_c-\zeta)^n}{n!}\frac{\partial^n\Delta\mathcal{P}_N(\zeta)}{\partial\zeta^n}, \tag{23}$$

$$\Delta\mathcal{P}_\zeta(N)=\sum_{n=0}^{\infty}\frac{(N_c-N)^n}{n!}\frac{\partial^n\Delta\mathcal{P}_\zeta(N)}{\partial N^n}. \tag{24}$$

The discontinuous $\frac{\partial^n f(x)}{\partial x^n}$ at the critical point denotes the nth-order phase transition.

III. SECOND-ORDER PHASE TRANSITION IN THE CHIRAL LIMIT

A. Divergent peak of χ^c

After solving the above coupled DSEs in the rainbow approximation by means of the iteration method, we can obtain the three functions A, B, and Π for the propagators and the interrelated functions C, D, Π' for the scalar

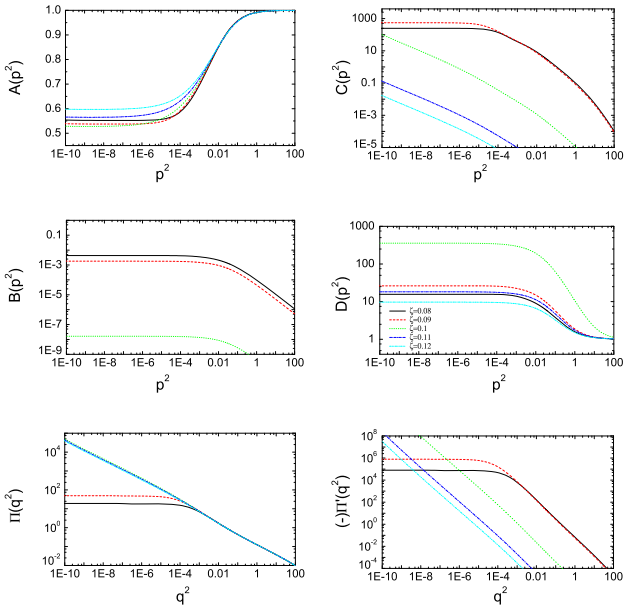

FIG. 1. The typical behavior of $A(p^2)$, $C(p^2)$, $B(p^2)$, $D(p^2)$, $\Pi(p^2)$, and $-\Pi'(q^2)$ with several values of ζ near ζ_c at $N=1$.

susceptibility. The numerical results are plotted in Figs. 1 and 2 at fixed N and ζ, respectively.

From Figs. 1 and 2, it is found that, at small ζ or N, the fermion self-energy equation has a nonzero solution. Based on the CJT effective potential [33], the potential of the Wigner phase [where $B(p^2)\equiv 0$] is larger than that of the Nambu phase [with $B(p^2>0)$] and hence the DCSB occurs. In this phase, $A(p^2)$ and $D(p^2)$ approach 1 at large p^2 while the other functions vanish in the large-momentum limit, and all six functions are almost constant in the

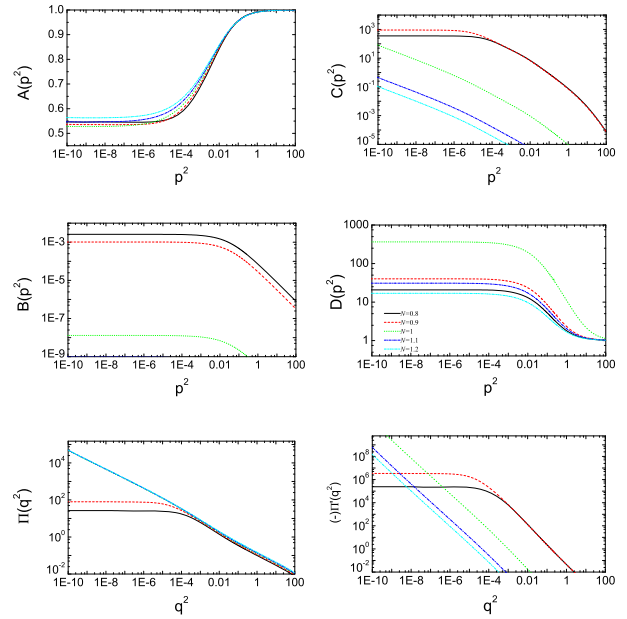

FIG. 2. The typical behavior of $A(p^2)$, $C(p^2)$, $B(p^2)$, $D(p^2)$, $\Pi(p^2)$, and $-\Pi'(q^2)$ with several values of N near N_c at $\zeta=0.1$.

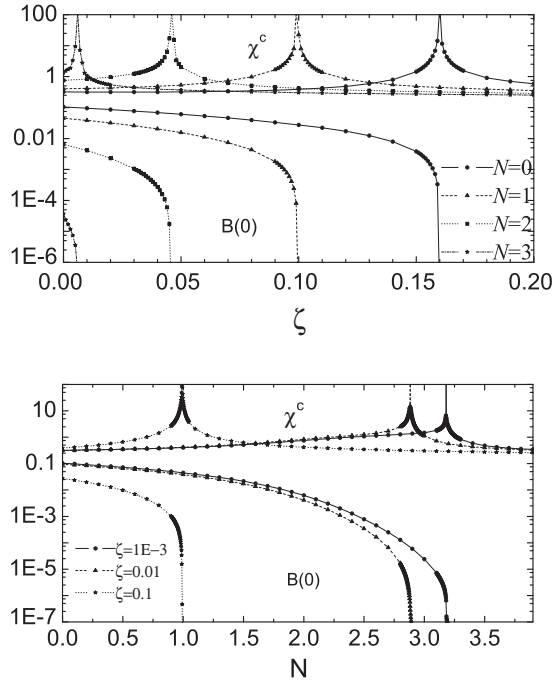

FIG. 3. The divergent peak of the chiral susceptibility and the vanishing $B(0)$ around the critical points with several values of N (top) and ζ (bottom).

infrared region. Based on Eq. (3), $B(0)$ can also be treated as an order parameter of the CPT. As ζ or N increases, $B(0)$ decreases at a critical value ζ_c or N_c, while $D(0)$ increases and in fact reveals its divergent behavior at this point. With increasing ζ or N, the gap equation (15) has only one trivial solution, i.e., $B(p^2) \equiv 0$ and the chiral symmetry is restored. Here, the vanishing $B(0)$ corresponds to the infinite $\Pi(0)$. However, A and C reveal their abnormal behaviors in the chiral-symmetric phase. $A(p^2)$ at small p^2 remains almost constant which is obviously different from the case with $\zeta = 0$ [34], while $C(p^2)$ is divergent in the infrared region.

Substituting the above four functions A, B, C, and D, we obtain the chiral susceptibility with a range of ζ and N and illustrate them in Figs. 3 and 4. The upper lines in Fig. 3 illustrate the behavior of the chiral susceptibility and the lower lines in this figure show the infrared value of $B(p^2)$. As is shown in Fig. 3, for any given N, χ^c stays almost constant for small and large ζ, while it shows an apparent peak at some critical boson mass which depends on N and decreases as N increases. This result is consistent with our previous work [21] in which the fermion chiral condensate was adopted to gain the curve of the CPT in the (ζ, N) plane. It is well known that the nature of a phase transition is a very important and basic issue in the study of phase transitions and the chiral susceptibility is an effective parameter to study the features of the chiral phase transition. As shown below, with the involved nonzero boson mass, the CPT is a typical second-order phase transition.

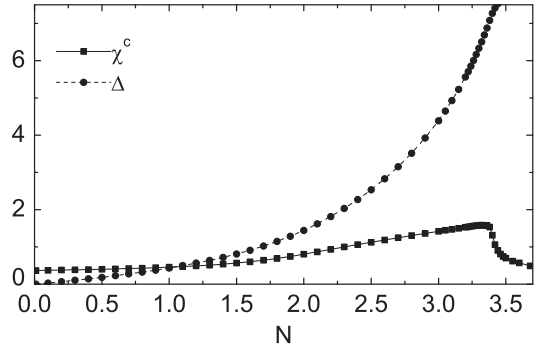

FIG. 4. The dependence of the chiral susceptibility and $B(0)$ on N at $\zeta = 0$. (Here, $\Delta = -\ln\frac{B(0)_N}{B(0)_{N=0}}$.)

We see that, at any N, the peak of the susceptibility lies at ζ_{Nc} and exhibits a very narrow, pronounced, and in fact divergent peak, which also reveals a typical characteristic of the second-order phase transition driven by the restoration of chiral symmetry. For a fixed ζ, with increasing N, chiral symmetry is restored at a critical $N_{\zeta c}$ and the susceptibility exhibits the same behavior around the critical point. From Fig. 3, we see that the chiral susceptibility reveals its infinite value at $N_{\zeta c}$, which also illustrates the typical second-order phase transition.

By means of the same method, we also obtain the value of the chiral susceptibility and $B(0)$ with a range of fermion flavors with zero boson mass. The results are plotted in Fig. 4. From this figure, we see that as N increases the chiral susceptibility shows an obvious peak, while $B(0)$ vanishes. In addition, we also see that the susceptibility around N_c is apparently different from that with a nonzero boson mass where the peak shows neither a divergent nor a discontinuous behavior, which illustrates that the CPT at N_c with zero boson mass is neither of first order nor of second order and thus is a higher-order continuous phase transition.

As is well known, the massless boson mediates the long-range interaction, while the massive boson mediates the short-range interaction. This effect is clearly illustrated in Fig. 1. Just as shown in Fig. 1, the fermion self-energy is depressed by the nonzero mass of the boson. It is precisely this depression given by the boson mass that changes the characteristic of the chiral phase transition of the system: the chiral phase transition with a massive boson reveals the typical second-order phase transition, while exhibiting a higher than second-order transition at the critical number of fermion flavors in the case of a massless boson.

B. Results from the CJT effective potential

If we substitute different solutions of A, B, and Π in both DCSB and the chiral-symmetric phase, we can also obtain the differential pressure and its derivative change with the variation of N or ζ. Their behavior can be seen in Figs. 5 and 6. We find that each of the three functions $\Delta\mathcal{P}$, $\Delta\mathcal{P}'$,

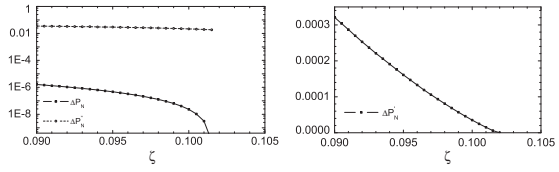

FIG. 5. The dependence of $\Delta\mathcal{P}_N, \Delta\mathcal{P}''_N(=\frac{\partial^2\Delta\mathcal{P}}{\partial\zeta^2})$ (left) and $\Delta\mathcal{P}'_N(=-\frac{\partial\Delta\mathcal{P}}{\partial\zeta})$ (right) on ζ near the critical boson mass at $N=1$.

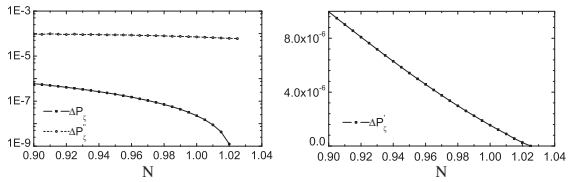

FIG. 6. The dependence of $\Delta\mathcal{P}_\zeta, \Delta\mathcal{P}''_\zeta(=\frac{\partial^2\Delta\mathcal{P}}{\partial N^2})$ (left), and $\Delta\mathcal{P}'_\zeta(=-\frac{\partial\Delta\mathcal{P}}{\partial N})$ (right) on N near the critical number of fermion flavors at $\zeta=0.1$.

and $\Delta\mathcal{P}''$ falls with increasing ζ (or N) and $\Delta\mathcal{P}, \Delta\mathcal{P}'$ decrease monotonically to zero at the critical boson mass ζ_{Nc} (or the critical number of fermion flavors $N_{\zeta c}$) which corresponds to the vanishing point of the fermion chiral condensate. The diminishing $\Delta\mathcal{P}'$ illustrates that the CPT at the critical point is not a first-order phase transition.

We also see that $\Delta\mathcal{P}''$ in the DCSB phase exhibits a continuous behavior with the alteration of ζ and N but jumps to zero at the critical point. The jumping behavior of $\Delta\mathcal{P}''$ shows that the system in the original chiral symmetry breaking phase undergoes a second-order phase transition into the chiral-symmetric phase.

However, when ζ decreases, the nature of the CPT near the critical number of fermion flavors exhibits different behavior. We can also obtain how the differential pressure and its derivatives change with the variation of N, which we illustrate in Fig. 7. From Fig. 7, it can be seen that all three functions $\Delta\mathcal{P}_N, \Delta\mathcal{P}'_N$, and $\Delta\mathcal{P}''_N$ fall monotonically to zero as N increases and the curves show no jump near the critical number of fermion flavors. This means that the transformation from the DCSB phase to the chiral-symmetric phase is neither of first order nor of second order, but rather should be a higher-order continuous phase transition. This is the same as the result for the chiral susceptibility.

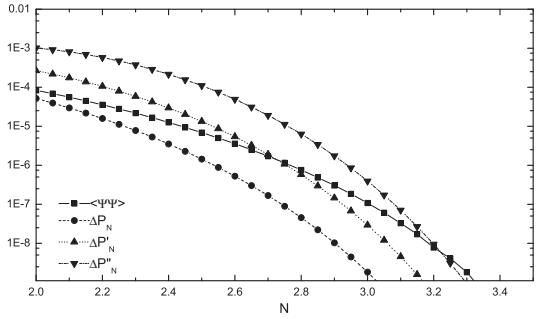

FIG. 7. The dependence of $\Delta\mathcal{P}_N, \Delta\mathcal{P}'_N$, and $\Delta\mathcal{P}''_N$ at $\zeta=0$ in the DCSB phase.

IV. CROSSOVER BEYOND THE CHIRAL LIMIT

To indicate the transition in the case of the nonchiral limit, we also investigate the peak of the chiral susceptibility and plot its typical behavior with a series of values of ζ at a fixed N in Fig. 8. From Fig. 8 we see that, as the gauge boson mass increases, the chiral susceptibility exhibits an apparent peak, but the corresponding value of ζ changes little with the increasing fermion mass. Nevertheless, the chiral susceptibility depends little on ζ and the fermion mass at small and large ζ. Moreover, we find that—as distinguished from the case in the chiral limit—the susceptibility exhibits nonsingular behavior at finite fermion masses. The peak of the susceptibility becomes smooth and its height is greatly suppressed and evidently finite; thus, there is no unique value of ζ, but rather a range of finite width where the transition phenomenon appears.

Similarly, we also obtain the typical behavior with a range of N at a fixed ζ, which we show in Fig. 9. One finds that, beyond the chiral limit, the susceptibility exhibits a smooth peak and the value of the peak falls with increasing fermion mass; it either has not a unique value of N to undergo the transition phenomenon.

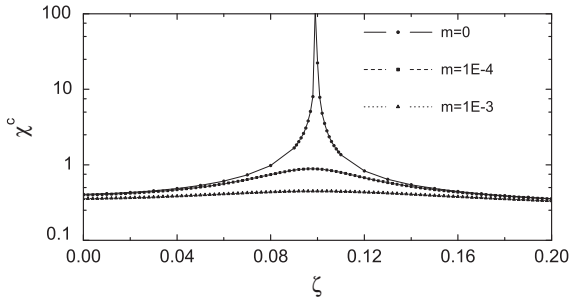

FIG. 8. The relation between the chiral susceptibility and ζ at several values of m when $N=1$.

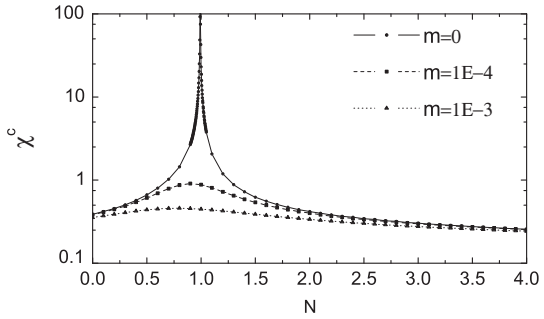

FIG. 9. The relation between chiral susceptibility and N at several m when $\zeta=0.1$.

V. CONCLUSIONS

The goal of this paper was to investigate the nature of the chiral phase transition of QED_3 at zero temperature through a continuum study of the chiral susceptibility and the CJT effective potential, with zero/nonzero boson mass near the critical values, including the critical number of fermion flavors and critical boson mass.

With a nonzero boson mass, the chiral susceptibility at either the critical number of fermion flavors or critical boson mass shows large and in fact divergent peaks, which illustrates a typical characteristic of a second-order phase transition driven by chiral symmetry restoration in QED_3 at zero temperature. To check the conclusion, we also adopted the Cornwall-Jackiw-Tomboulis effective potential framework to analyze the nature of the *CPT* with a nonzero boson mass. The general method shows that the second-order partial derivative of the pressure difference about ζ or N jumps to zero at the critical point, which gives an obvious proof of the second-order transition. Nevertheless, in the absence of a boson mass at zero temperature around the critical number of fermion flavors, the chiral susceptibility exhibits a smooth and finite peak, and the first and second order partial derivatives of N of the differential pressure monotonously decrease. The behavior of the two parameters shows that QED_3 with zero boson mass undergoes a higher than second-order phase transition at the critical number of fermion flavors.

On the other hand, considering a finite fermion mass, the chiral susceptibility exhibits a smooth peak, which changes in an N or ζ range of smooth width and also reveals its stressed peak with increasing fermion mass: this behavior indicates a typical crossover beyond the chiral limit in the Anderson-Higgs model.

ACKNOWLEDGMENTS

We would like to thank Prof. Wang Qiang-hua and C. D. Roberts for their helpful discussions. This work is supported in part by the National Natural Science Foundation of China under Grants Nos. 11275097, 11475085, and 11535005, and by the Fundamental Research Funds for the Central Universities (under Grant No. 2242014R30011).

[1] P. Maris, Phys. Rev. D **52**, 6087 (1995).
[2] G. Grignani, G. Semenoff, and P. Sodano, Phys. Rev. D **53**, 7157 (1996).
[3] P. Maris, Phys. Rev. D **54**, 4049 (1996).
[4] C. J. Burden, J. Praschifka, and C. D. Roberts, Phys. Rev. D **46**, 2695 (1992).
[5] A. Bashir, A. Raya, I. C. Cloet, and C. D. Roberts, Phys. Rev. C **78**, 055201 (2008).
[6] W. Rantner and X. G. Wen, Phys. Rev. Lett. **86**, 3871 (2001).
[7] M. Franz and Z. Tesanovic, Phys. Rev. Lett. **87**, 257003 (2001).
[8] I. F. Herbut, Phys. Rev. Lett. **88**, 047006 (2002); Phys. Rev. B **66**, 094504 (2002); Phys. Rev. Lett. **94**, 237001 (2005).
[9] X. G. Wen and A. Zee, Phys. Rev. Lett. **69**, 1811 (1992).
[10] G. Z. Liu and G. Cheng, Phys. Rev. B **66**, 100505 (2002).
[11] T. Appelquist, D. Nash, and L. C. R. Wijewardhana, Phys. Rev. Lett. **60**, 2575 (1988).
[12] D. Nash, Phys. Rev. Lett. **62**, 3024 (1989).
[13] C. S. Fischer, R. Alkofer, T. Dahm, and P. Maris, Phys. Rev. D **70**, 073007 (2004).
[14] J. S. Ball and T. W. Chiu, Phys. Rev. D **22**, 2542 (1980).
[15] D. C. Curtis and M. R. Pennington, Phys. Rev. D **42**, 4165 (1990).
[16] T. Appelquist, D. Nash, and L. C. R. Wijewardhana, Phys. Rev. Lett. **60**, 2575 (1988).
[17] T. Appelquist, J. Terning, and L. C. R. Wijewardhana, Phys. Rev. Lett. **75**, 2081 (1995).
[18] H. T. Feng, B. Wang, W. M. Sun, and H. S. Zong, Phys. Rev. D **86**, 105042 (2012).
[19] H. T. Feng, J. F. Li, Y. M. Shi, and H. S. Zong, Phys. Rev. D **90**, 065005 (2014).
[20] G. Z. Liu and G. Cheng, Phys. Rev. D **67**, 065010 (2003).
[21] H. T. Feng, W. M. Sun, F. Hu, and H. S. Zong, Int. J. Mod. Phys. A **20**, 2753 (2005).
[22] J. M. Cornwall, R. Jackiw, and E. Tomboulis, Phys. Rev. D **10**, 2428 (1974).
[23] T. Itoh, Y. Kim, M. Sugiura, and K. Yamawaki, Prog. Theor. Phys. **93**, 417 (1995).
[24] H. Kleinert, F. S. Nogueira, and A. Sudbo, Nucl. Phys. **B666**, 361 (2003).
[25] G. Z. Liu and G. Cheng, Phys. Rev. B **65**, 132513 (2002).
[26] E. Fradkin and S. H. Shenker, Phys. Rev. D **19**, 3682 (1979).
[27] J. F. Li, F. Y. Hou, Z. F. Cui, H. T. Feng, Y. Jiang, and H. S. Zong, Phys. Rev. D **90**, 073013 (2014).
[28] H. T. Feng, Mod. Phys. Lett. A **27**, 1250209 (2012).
[29] X. Z. Wang, J. F. Li, X. H. Yu, and H. T. Feng, Chin. Phys. Lett. **32**, 111102 (2015).
[30] J. F. Li, H. T. Feng, Y. Jiang, W. M. Sun, and H. S. Zong, Mod. Phys. Lett. A **27**, 1250026 (2012).
[31] N. Brown and M. R. Pennington, Phys. Rev. D **39**, 2723 (1989).
[32] C. J. Burden, J. Praschifka, and C. D. Roberts, Phys. Rev. D **46**, 2695 (1992).
[33] P. L. Yin, Z. F. Cui, H. T. Feng, and H. S. Zong, Ann. Phys. (Amsterdam) **348**, 306 (2014).
[34] H. T. Feng, M. He, W. M. Sun, and H. S. Zong, Phys. Lett. B **688**, 178 (2010).